Proceedings of ICONE 9
9th International Conference on Nuclear Engineering
April 8-12, 2001, Nice, France

EFFECT OF THE IN- AND EX-VESSEL DUAL COOLING ON THE RETENTION OF AN INTERNALLY HEATED MELT POOL IN A HEMISPHERICAL VESSEL

K.I. AHN, B.S. KIM, D.H. KIM

Thermal Hydraulic Safety Research
Korea Atomic Energy Research Institute
Dukjin-Dong 150, Yusong-Ku, Taejon, 305-353, KOREA
Fax: 82-42-868-8256, e-mail: *kiahn@kaeri.re.kr*

Key Words: Severe Accidents, In-vessel Melt Retention (IVMR), In- and Ex-vessel Dual Cooling

A concept of in-vessel melt retention (IVMR) by in-vessel reflooding and/or reactor cavity flooding has been considered as one of severe accident management strategies and intensive researches to be performed worldwide. This paper provides some results of analytical investigations on the effect of both in- / ex-vessel cooling on the retention of an internally heated molten pool confined in a hemispherical vessel and the related thermal behavior of the vessel wall. For the present analysis, a scale-down reactor vessel for the KSNP reactor design of 1000 MWe (a large dry PWR) is utilized for a reactor vessel. Aluminum oxide melt simulant is also utilized for a real corium pool. An internal power density in the molten pool is determined by a simple scaling analysis that equates the heat flux on the the scale-down vessel wall to that estimated from KSNP. Well-known temperature-dependent boiling heat transfer curves are applied to the in- and ex-vessel cooling boundaries and radiative heat transfer has been only considered in the case of dry in-vessel. MELTPOOL, which is a computational fluid dynamics (CFD) code developed at KAERI, is applied to obtain the time-varying heat flux distribution from a molten pool and the vessel wall temperature distributions with angular positions along the vessel wall. In order to gain further insights on the effectiveness of in- and ex-vessel dual cooling on the in-vessel corium retention, four different boundary conditions has been considered: no water inside the vessel without ex-vessel cooling, water inside the vessel without ex-vessel cooling, no water inside the vessel with ex-vessel cooling, and water inside the vessel with ex-vessel cooling.

INTRODUCTION

One of the most important issues arising in the analysis of severe core melt accidents, is to predict accurately the possibility of in-vessel melt retention (IVMR) through the removal of the decay heat generated in the molten corium from the lower head of the RPV, by either the in-vessel reflooding or the reactor cavity flooding. The possibility of IVMR depends on the heat flux at the inner side of the vessel (between melt and wall), the heat transfer at the upper side of the melt (between melt pool and upper boundary), the heat conductivity of the vessel material and the heat transfer at the outer side of the wall (between wall and boiling water). Among thses, the downward heat transfer from the melt pool to the peripheral crust region has the firsthand impact on the conduction heat flux out to the reactor lower head which, in turn, determine damage to the lower head wall. Various heat transfer mechanisms should be considered to investigate this issue, including natural convection of a molten pool which governs the heat

flux distribution on the vessel wall, thermal interaction between the molten pool and the vessel wall which takes into account the process of vessel melting, possibility of in-vessel cooling by different cooling regimes of the molten pool upper boundary and external cooling of the reactor walls by the flooding of the reactor cavity, and mechanical behavior of the vessel. For a successful IVMR, it should prove that the heat transfer is efficient enough so that at least part of the RPV wall thickness maintains its structural properties and is able to support the mechanical load that results both from the weight of the corium and the lower head, and from pressure difference inside and outside the RPV.

The in-vessel cooling can be made possible by an accident mitigation action like a passive in-vessel water injection to cool down molten or particulate debris accumulated in the vessel lower head during a late core degradation phase. In spite of several adverse effects like significant hydrogen generation and corium-coolant interactions of various strength, in-vessel water injection to cool down the lower head debris bed is still recognized as an important and generally reliable measure for all cases where knowledge on the lower head core material interactions is insufficient. In constrast, the ex-vessel cooling has been regarded as one of IVMR strategies, by keeping the temperature of a significant portion of the RPV lower head below the wall creep deformation criteria. Intensive researches have been performed worldwide on the feasibility of IVMR through an external cooling of the reactor lower head as one of possible accident management strategies [1-6]. In reactor cases, it has been shown that the small and medium-sized reactor design could maintain the integrity of the reactor lower head during a severe core melt accident [3]. When much higher heat flux through the vessel is considered, however, there is no evidence that external cooling can extract the decay heat from the in-vessel corium. The efficiency of ex-vessel cooling should be further investigated to explore the feasibility of in-vessel corium retention, particularly for reactor vessels with high volumetric heating rate.

Compared with the ex-vessel cooling only, a concept of in-vessel gap cooling supported by the ex-vessel cooling has been expected to enhance the efficiency of heat removal from the molten pool to the cooling boundaries or for a successful IVMR [7]. In case that there is no contact resistance gap between the molten pool crust and the vessel inner wall, however, fewer studies have been performed for the effect of in- and ex-vessel dual cooling on the RPV thermal behavior yet. The main purpose of this paper is to investigate analytically the effect of both in- / ex-vessel cooling on the retention of an internally heated hemispherical molten pool in the absence of in-vessel gap cooling. In the present analysis, a scale-down reactor vessel for the Korean Standard Nuclear Power Plant (KSNP, a large dry PWR of 1000 MWe) adopting the ex-vessel cooling strategy [8] is utilized for reactor vessel. Aluminum oxide simulant is also utilized for a real corium pool. In that case, an internal power density in the molten pool can be determined by a simple scaling analysis that equates the heat flux on the scale-down vessel wall to estimate from the referenced reactor. Well-known temperature-dependent boiling heat transfer curves are applied to the in- and ex-vessel cooling boundaries. A computational fluid dynamics (CFD) code developed at KAERI, MELTPOOL, is applied to obtain the time-varying heat flux distribution from a molten pool and the vessel wall temperature distributions with angular position along the vessel wall. The MELTPOOL code simulates conjugate problems including natural convection heat transfer in the molten pool, heat conduction in the vessel wall, and in- and ex-vessel cooling under pool boiling condition. In the previous studies [9,10], the effectiveness of the MELTPOOL model has been well verified through the analysis of the partial solidification of a melt pool with/without volumetric heat sources and boundary cooling by water, especially for laminar flow regime of a molten pool. In order to gain further insights on the effectiveness of in- and ex-vessel dual cooling on the in-vessel corium retention, the present results are compared with results obtained for each of four different boundary conditions: no water inside the vessel without ex-vessel cooling, water inside the vessel without ex-vessel cooling, no water inside the vessel with ex-vessel cooling, and water inside the vessel with ex-vessel cooling. It should be noted that no other types of cooling mechanisms are considered through a gap between the melt pool crust and the hemispherical wall even though its effectiveness for heat removal has been proven in some cases of experimental and analytical studies. Regarding melting of the vessel wall,

no local convection that is expected to enhance heat removal to the outer region of the wall is considered for the melted portions of the wall. In addition, mechanical failure due to the vessel thermal stresses or creep is not considered.

BRIEF DESCRIPTION OF MELTPOOL MODELS

The current version of MELTPOOL has the capabilities of analyzing laminar convection of a single component fluid with volumetric heat generation, solid-liquid phase change of fluid, heat conduction in a hemispherical vessel wall containing the fluid, pool boiling convection and radiation heat removal through the fluid boundaries.

Molten Pool Thermal Behavior Model

The following assumptions are employed in the presnet analytical model to describe a molten pool thermal behavior :

(1) The liquid molten pool material is subjected to a single species with a uniform heat source.
(2) The flow type is axisymmetric, laminar, incompressible, and Newtonian. The material properties remain fixed at constant during the whole transient time. Density is also constant in all terms of the governing equations except a buoyancy term, because thermal expansion is explicitly included (i.e., the Boussinesq approximation).
(3) An enthalpy formulation for the energy equation is used to account for phase changes.
(4) Heat conduction is only considered in the vessel wall when the wall is partially molten.

Under the aforementioned conditions, the conservation equations are given as,

Conservation of mass

$$\nabla \cdot \mathbf{u} = 0 \tag{1}$$

Conservation of momentum

$$\rho_{ref}\left(\frac{\partial \mathbf{u}}{\partial t} + (\mathbf{u}\cdot\nabla)\mathbf{u}\right) = -\nabla p + \nabla\cdot(\mu\nabla\mathbf{u}) + S_B + S_{\mathbf{u}} \tag{2}$$

Conservation of energy

$$\rho_{ref}\left(\frac{\partial h}{\partial t} + (\mathbf{u}\cdot\nabla)h\right) = \nabla\cdot[\kappa\nabla(h/c)] + S_q + S_h \tag{3}$$

Heat conduction in the vessel wall

$$\rho_{ref}\left(\frac{\partial h}{\partial t} + (\mathbf{u}\cdot\nabla)h\right) = 0 \tag{4}$$

Source terms

$$S_B = -\rho_{ref}\,g\beta(h-h_{ref})/c \tag{5a}$$

$$S_{\mathbf{u}} = -\frac{\mu}{K}\mathbf{u} \tag{5b}$$

$$S_h = -\rho_{ref} L\left(\frac{\partial f}{\partial t} + (\mathbf{u}\cdot\nabla)f\right) \tag{5c}$$

Here the buoyancy source term, S_B, accounts for the natural convection effects of the melt pool. The velocity source terms, $S_{\mathbf{u}}$, are used to suppress or initiate the velocity components as the liquid material undergoes a phase change from a liquid state to a solid state or vice-versa. The energy source term, S_h, is

used to account for the effect of solidification and the related liquid fraction f is defined as $\Delta H / L$. For example, the first transient term of S_h describes the energy released from the liquid phase when solidification is made and the second term accounts for the convective effects due to the presence of a mushy region (if this exists). Finally, the volumetric heat source term is given as S_q.

In order to evaluate the flow and enthalpy fields, the above set of coupled partial differential equations (PDEs) is discretized on non-orthogonal grids using a finite volume approach with collocated arrangements of variables. The boundary-fitted non-orthogonal grids are most often used to calculate flows in complex geometries [11]. The advantage of such grids is that they can be adapted to any geometry, as optimum properties are easier to achieve than with non-orthogonal curvilinear grids. Accordingly, the problems varying with the depth of a melt pool can be solved. The discretized equations are solved iteratively using the strongly implicit procedure (SIP) of Stone [12] and the SIMPLEC algorithm [13]. The second order Euler backward implicit time stepping with stability at a large time step is employed for constructing the discretization equations for unsteady flow and enthalpy. The iterative procedure for obtaining the velocity and enthalpy field is repeated to determine the evolution of the solidification with time within each time step until convergence is satisfied. The central difference scheme (CDS) using deferred correction is utilized to discretize the convective term of the momentum equation. In cells that are undergoing a phase change, the condition that all velocities in solid regions are zero was made by gradually reducing the velocities from a finite value in the liquid to zero in the full solid over the computational cells. This can be achieved by assuming that such cell behaves as a porous medium containing a mixture of solid and liquid and appropriately defining a permeability in the Darcy source terms. Also, the liquid fraction at n-th iterative step is applied as a function of temperature in the energy equation. A main drawback to this approach is that the predicted enthalpy may oscillate above and below $c \cdot T_m$ and the $f \cdot L$ value is expected to oscillate between 0 and L. In this case, convergence will not be achieved. To ensure that no serious oscillations occur in the predicted enthalpy values from one iteration to the next, the liquid fraction correction approach [14] was used to treat this source term during an iterative solution step of the enthalpy equation. More details of numerical methods used in the present model are well described in Reference 9.

Upward Boundary Cooling Model

The upper surface of the melt pool may be cooled by its overlying water (i.e., wet condition) or subjected to dry atmosphere (i.e., dry condition). For a dry condition, a constant heat transfer coefficient is utilized in the present model. However, boiling heat transfer is assigned for the upper surface of the molten pool filled with a water pool. For example, the *Rohsenow* correlation [15] is considered for a nucleate boiling regime and a modified *Bromley* correlation [16] is employed for a film boiling regime. Also, critical and minimum heat fluxes were calculated with the *Zuber* correlation [17]. If neither of these conditions are met, the surface is in transition boiling and a logarithmic interpolation between the critical heat flux (CHF) and the minimum film boiling heat flux for the surface temperature of the molten pool is used to determine the heat flux at that temperature. For all the above cases, once a heat flux has been determined, an effective heat transfer coefficient is evaluated as the ratio of heat flux over the difference between the molten pool surface and the water pool temperatures. This heat transfer coefficient is used as the boundary heat transfer coefficient in the solidified upper surface. On the other hand, radiation heat transfer between a melt pool surface and an overlying water pool is calculated during stable film and transition boiling.

Downward Boundary Cooling Model

The vessel outside region may be submerged in water (i.e., wet condition) or subjected to the atmosphere (i.e., dry condition). For a dry condition, a constant heat transfer coefficient is utilized in the present

model. For a wet condition, however, the heat transfer coefficients for natural convection, nucleate, transition, and film boiling at different outer wall temperatures are utilized to calculate the heat loss from the wall submerged in the water pool. These are determined by the temperature of the vessel outer wall. For subcooled water, for example, the present model utilizes the average single phase natural convection heat transfer coefficient for a submerged hemisphere which is obtained from the correlation suggested by Churchill & Churchill [17]. Also, the heat transfer coefficients in nucleate and transitional boiling are obtained by two correlations based on the experimental results of Dhir [18]. The heat transfer rate in the film boiling region is much less than that in the nucleate boiling region. In that case, a minimum film boiling is conservatively assumed in the present model. If the water conditions are different from the above cases, correlations used in the upward boundary cooling condition are utilized. The present cooling model is only applied to the pool boiling condition, and the characteristics of bubble formation on the hemishperical surface. Bubble behavior along the curved surface (i.e., two-phase hydrodynamics) is not taken into account to obtain heat transfer at the surface.

NUMERICAL INVESTIGATIONS

Figure 1 shows a schematic of the molten pool configuration and boundary cooling conditions considered for the present analysis.

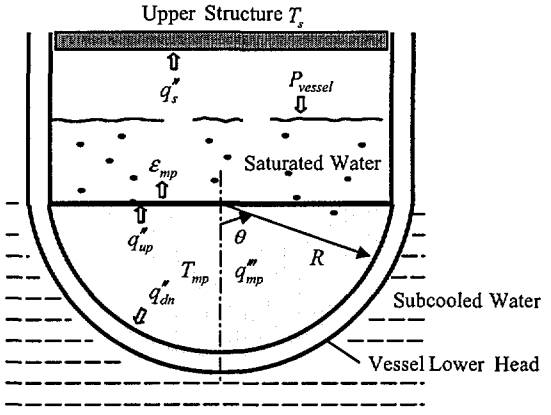

Fig.1. Schematic of the Hemishperic Pool and Boundary Cooling Conditions

Initial Configuration of Molten Pool

In the present analysis, it is assumed that the scale-down vessel lower head with an inner radius of 0.25 m is fully filled with Al_2O_3 melt simulant (with Prandtle number of 0.68) in place of a molten corium pool (with Pr number of 0.5 ~ 0.8) and various constituents of the core material are mixed homogeneously in the vessel lower head. These geometrical and molten pool conditions have been utilized in the LAVA-4 gap-cooling experiment [19] of the SONATA experimental series [20]. Since the Pr number is an indicator of physical properties of working fluids, the physics of the heat transfer process under prototypical conditions of interest can be generalized to the reactor material with similar Pr number. Also, it is assumed that the molten pool and crust are subjected to the same material properties. The initial temperature of the vessel wall is assumed to be 427 K at all locations in the wall. However, it should be noted that the transient vessel temperatures are not sensitive to the assumed value of the initial temperature of the wall. Regarding melting of the vessel wall, no local convection that is expected to enhance heat removal to the outer region of the wall is considered for the melted portions of the wall.

In a scale-down reactor vessel, it is necessary to specify an appropriate heat source comparable with a typical reactor case. In order to reflect a similar thermal load on the vessel wall, an amount of power density generated in the molten pool (via an external heating method such as direct electrical or Joule heating) is determined by equating heat flux in the scale-down vessel to that estimated from a typical reactor case. The internal heat generation can be estimated by the following overall heat balance that equates the heat production rate from a hemispheric pool to the heat loss rate through its surfaces [3,21] (see Nomenclature) :

$$\overline{q}''_{dn} = q''' V_{mp} \{2\pi R^2 (1 + 0.5R')\}^{-1}, \tag{6}$$

$$q''' = (S_{up}\overline{q}''_{up} + S_{dn}\overline{q}''_{dn}) / V_{mp},\ V_{mp} = \frac{2}{3}\pi R^3 \ \text{for}\ H/R = 1.0, \tag{7}$$

$$R' = Nu_{up} / Nu_{dn}, \tag{8}$$

Here, the ratio of the up-to-down heat fluxes, R' , depends on the Rayleigh number (Ra') and the strength of natural convection occurring within the molten pool. For example, the heat flux corresponding to the decay heat is about 0.6 MW/m^2 for the KSNP design with the electricity power of 1000 MWe (thermal power of 3000 MW$_{th}$) and with the RPV inner radius of 2.06 m. For a full depth of molten corium without natural convection, the aforementioned condition of KSNP gives the decay heat of about 24 MW in the reactor lower head (i.e., decay power density of 1.3 MW/m^3 for R'=1.0 and 1.43 MW/m^3 for R'=1.3). For the present scale-down reactor vessel (R=0.25m), the internal power density of 10.8 MW/m^3 in the case without natural convection (i.e., R'=1.0) or 11.8 MW/m^3 in the case with natural convection (R'=1.3) is required to generate the same heat flux as that of the KSNP. In this analysis, we utilize a lower power density of 10 MW/m^3 corresponding to the lower bound of internal power density. This heat source is characterized by the Rayleigh number of 6.5×10^{10} in the present scale-down geometry and the value is much lower than that of a real corium expected in the core meltdown accident (c.f., $10^{14}\sim10^{17}$). Since the Ra number is the only representative dimensionless group of natural convection heat transfer, at least, for the fluids with constant physical properties, that is, the present condition is expected to give a stronger effect of natural convection heat transfer (or thermal stratification), compared with that of a real corium. The present value of Rayleigh number belongs to a laminar-to-turbulence transient regime of natural convection flow under a given Prandtle number (0.68). No special turbulence models might be used up to a Ra number of 10^{12} [22].

Upper and Lower Boundary Conditions

For dry case, the heat from the upper surface of the molten pool is transported by radiation mainly, which is a strong function of the temperature. In the present analysis, the radiation heat transfer to the upper structure is calculated by assuming the upper structure temperature of 427 K (same as the initial temperature of the vessel wall), and the back radiation which is reflected or radiated from the upper structure of the vessel to the molten pool is neglected. The emissivity in the upper surface of the molten pool is assumed to be 0.6 (c.f., 0.4 ~ 0.5 in the case of molten corium) and the emissivity of the vessel outer wall is neglected due to a small temperature difference between the vessel outer wall and the surrounding atmoshpere.

In the case of ex-vessel cooling, it is assumed that water is submerged in the entire outer surface of the vessel lower head prior to the slumping of corium and its temperature is maintained constant (subcooling of 50 K at 1 bar) over the whole transient time. The initial temperature of the molten pool is assumed to be 2500 K (180 K superheat). A cooling water of 427 K is applied for in-vessel cooling (i.e., saturation temperature at given system pressure 17 bar) and its temperature remains constant over the whole transient time. In the case of in- or ex-vessel cooling, temperature-dependent heat transfer coefficients are applied to calculate the heat loss into the water, e.g., single phase natural convection, nucleate, transition, and film boiling. However, the feedback effect of thermal hydraulic conditions due to sustained steam

generation and associated system pressurization is neglected in this study. Analyses are also not considered for the sufficient access of water to the bottom of the vessel lower head and venting of a steam/water mixture on the top, and dynamic behavior of the two-phase natural circulation flow. The aforementioned phenomena causes a periodic bubble formation and detachment mechanism at the position of horizontal tangency on the vessel lower head in combination with the large thermal inertia of it allows very significant margins to critical heat flux (CHF).

Numerical Results and Discussion

Based on the aforementioned conditions, a set of calculational materix was prepared for the present analysis and it is summarized in Table 1. Thermophysical properties for the melt pool simulant and the vessel wall are also given in Table 2. Under different cooling conditions of the melt pool boundaries, the following four test cases were analyzed :

(1) no water inside the vessel without ex-vessel cooling (dry in-vessel and dry ex-vessel);
(2) water inside the vessel without ex-vessel cooling (wet in-vessel and dry ex-vessel);
(3) no water inside the vessel with ex-vessel cooling (dry in-vessel and wet ex-vessel);
(4) water inside the vessel with ex-vessel cooling (wet in-vessel and wet ex-vessel).

Calculations were carried out up to 2500 seconds and as the result the local heat fluxes and temperature transients at the vessel wall with three typical angular positions along the vessel wall were obtained.

Table 1 Initial & Boundary Conditions Used in the Present Analysis

Lower Head Geometric Conditions	Melt simulant: Al_2O_3 LH Inner Radius: 0.25 m Vessel wall thickness: 0.025 m
Molten Pool Initial Conditions - System pressure (bar) - Pool depth or Aspect ratio (H/R) - Initial melt pool temperature (K) - Melt pool heat source (MW/m^3) - Prandtl number of melt - Vessel wall temperature (K)	 17 1.0 2500 (180 K superheated) 10 ($Ra' = 6.75\times 10^{10}$) (cf. $Ra' \approx 10^{14}\sim 10^{17}$ for oxidic core melts) 0.68 (cf. Pr ≈ 0.6-0.8 for oxidic core melts) 427
Boundary Cooling Conditions - Melt pool overlying water (K) - Ex-vessel water temperature (K) - Ex-vessel HTC (dry case) - Temperature of upper structure (K)	 427 (saturation temperature at 17 bar) 323 (50 K subcooling at 1 bar) Constant HTC (50 W/m^2K) 427 K (initial temperature of the vessel wall)

Table 2 Thermophysical Properties Used in the Present Analysis

Thermophysical parameters	Melt Simulant : Al_2O_3	Vessel Wall : S/S
Melting temperature (K)	2320	1800
Latent heat of fusion (J/kg)	1.12×10^6	2.5×10^5
Specific heat ($J/kg\cdot K$)	1230	540
Thermal conductivity ($W/m\cdot K$)	9.0	35
Density (kg/m)	3751	8000
Dynamic viscosity ($kg/m\cdot s$)	5.0×10^{-3}	6.0×10^{-3}
Thermal diffusivity (m^2/s)	1.67×10^{-6}	-
Thermal expansion coefficient ($1/K$)	1.12×10^{-5}	1.0×10^{-4}
Thermal radiation emissivity	0.6	-

Molten Pool Thermal Behavior

Figure 1 shows a general trend of volume-averaged temperatures of the molten pool which is governed by a balance between the heat generation rate within the molten pool and the heat loss rate through the boundaries. If the rate of heat generation in the molten pool exceeds the radiative heat loss in the case of dry in-vessel or upward cooling condition in the case of wet in-vessel, the molten pool will freeze at its upper free surface. Otherwise, the molten pool upper surface will remain the initial liquid phase. Also, the initial temperature of the vessel inner wall is much lower than the freezing temperature of the molten pool and consequently a crust will begin to form on the inner wall of the vessel contacted with the molten corium immediately.

In the case of dry in-vessel and dry ex-vessel, after about 120 seconds the internal heat generation rate within the molten pool exceeds the heat loss rate to the molten pool boundary. Consequently, the average temperature of the molten pool (i.e., proportional to molten pool internal energy) begins to rise just after that time and eventually it reaches 2900 K at 2500 seconds. In the case of wet in-vessel and dry ex-vessel, the temperature rapidly increases up to the maximum temperature of 2780 K at 1250 seconds and thereafter it decreases continuously to a quasi-steady temperature of 2760 K that is much higher than the initial pool temperature. This quasi-steady temperature happens when the heat loss through the in-vessel cooling by the overlying water is equal to the heat generated inside the molten pool. Comparing with the case of dry in- and ex-vessel, the effect of in-vessel cooling in the absence of ex-vessel cooling only results in the corresponding molten pool temperature reduction of 120 K at 2500 seconds. When the ex-vessel cooling condition is imposed, the molten pool average temperature slowly decreases and after 1000 seconds it reaches quasi-steady temperatures of 2182 K in the case of dry in-vessel and of 2155 K in the case of dry in-vessel, respectively. Event though the ex-vessel cooling is highly effective in removing the heat from the molten pool in the vessel lower head, consequently, the effect of in- and ex-vessel dual cooling is not so much comparing with the ex-vessel cooling in the absence of in-vessel cooling,, i.e., a temperature reduction of 27 K in the quasi-steady state. The aforementioned result is mainly due that the upward facing boundary condition is more favorable for film boiling than for nucleate boiling under the present in-vessel cooling condition and in that case a main mechanism of the heat loss from the upper surface is thermal radiation like the case of dry in-vessel.

Table 3 Average Heat Flux Ratios at the Molten Pool Surfaces

Boundry conditions		Split fraction of surface-to-average heat fluxes		
In-vessel	Ex-vessel	$\overline{q}''_{up} / \overline{q}''_{avg}$	$\overline{q}''_{dn} / \overline{q}''_{avg}$	$\overline{q}''_{up} / \overline{q}''_{dn}$
Dry	Dry	2.78	0.11	25.3
Wet	Dry	2.87	0.10	28.7
Dry	Wet	1.41	0.80	1.76
Wet	Wet	1.47	0.77	1.91

Figures 2(a) through 2(d) show split fractions of surface-to-average heat fluxes and their approximate values at 2500 seconds are given in Table 3. As shown in Table 3, the ratio of the average upward-to-downward heat fluxes approaches to 1.8 in the cases of wet ex-vessel, but it highly diverses to near the value of 26 in the cases of dry ex-vessel. This means that the effect of natural convection in the molten pool is much stronger in the case of dry ex-vessel than in the case of wet ex-vessel, and consequently under the same molten pool configuration, much higher fraction of heat is transferred from the molten pool to the upper surface than to the curved surface. Similarly with the aforementioned molten pool temperature, however, the in-vessel cooling shows a small effect to the split fraction of the molten pool heat regardless of ex-vessel conditions.

Local Downward Heat Flux

Figures 3(a) and 3(b) show the variation of local heat flux for three different angular positions (0^o, 50^o, 80^o) at the outer wall, in the case of ex-vessel cooling. As given in the figures, the local downward heat flux ratio increases with angular position and it reaches the quasi-steady state much faster than the dry ex-vessel cases. In these cases, the vessel outside surface experiences subcooled nucleate boiling (with very high heat fluxes) and the local heat fluxes increase with angular position. That is, higher angular positions resulting in the corresponding higher heat fluxes. Here, it should be noted that in the case of the wet ex-vessel, the present nucleate boiling heat fluxes were calculated based on the Dhir's coorelation for nucleate boiling [18].

At any point on the outer wall, however, the local heat fluxes do not exceed the CHF values evaluated by the existing correlations of CHF. For example, the maximum local heat flux occurs at angular position of 80^o, which reaches 1.07 MW/m^2 in the case of in- and ex-vessel dual cooling and 1.03 MW/m^2 in the case of ex-vessel cooling alone, respectively. In addition, the corresponding steady state heat flux reaches 0.59 MW/m^2 in the case of in- and ex-vessel dual cooling and 0.61 MW/m^2 in the case of ex-vessel cooling alone, respectively. At the same angular point, the CHF values evaluated at the same point are subjected to 1.15 MW/m^2 in the case of the Zuber's flat-plate CHF correlation [23], 1.6 MW/m^2 in the case of ULPU experiments obtained in [3], and 1.8 MW/m^2 in the case of the Dhir's coorelation for nucleate boiling heat flux [18]. After all, the present local heat fluxes allow very significant margins to the speified CHF value. This fact is particularly important in view of the molten pool coolability or IVMR. When the heat flux through the vessel exceeds the CHF at the same location, boiling crisis occurs and in turn it results in a sudden transition of the flow regime from nucleate to film boiling. In that case, the corresponding heat transfer coefficient is considerably lower than that of nucleate boiling, and as a consequence the surface temperature rises to considerably higher values in order to accommodate the imposed thermal load from the inside. At such temperatures the vessel wall loses essentially all of its strength, and it becomes susceptible to creep, structure instability, and further melting. In this view of CHF, however, it is thus seen that the present downward heat fluxes from the molten pool are indeed removal and the vessel wall is coolable through nucleate boiling.

Vessel Wall Temperature Transient

Figures 4(a) through 4(c) show the variation of local temperature for three different angular positions (0^o, 50^o, 80^o) at the inner and outer walls of the hemispherical vessel. They reflect the dependence of the magnitude of the molten pool convective heat transfer on each of these angular positions. As shown in the figures, the lower vessel temperature profiles clearly exhibit the azimuthal dependency on the heat transfer from the molten pool (temperature increases along the azimuthal angle). A sizable temperature difference is also computed between the inner and outer walls of the vessel lower head. The substantial effect of ex-vessel cooling on thermal response of the vessel lower head is clearly explained by the following two results : (a) Regardless of in-vessel conditions, the entire vessel wall temperatures exceeded the melting point of the vessel (1800 K) just after about 300 seconds in the cases of dry ex-vessel ; (b) Regardless of in-vessel conditions, however, the entire vessel wall was maintained far below its melting temperature over the whole transient time in the cases of wet ex-vessel, with steady-state outer wall temperatures ranging from 474 K at 0^o to 489 K at 80^o and inner wall temperatures ranging from 824 K at 0^o to 1065 K at 80^o. The temperature difference between the outer side of the wall and the bulk of the water is also not so much in the cases of wet ex-vessel. Comparing with the ex-vessel cooling only, however, as shown in Figures 4(a) through 4(c), the effect of in- and ex-vessel dual cooling is minor in view of the vessel wall temperatures.

The aforementioned result can be explained by comparing the magnitude of heat ransfer coefficients evaluated in the upper surface of the molten pool and in the outer wall of the vessel, respectively, which depend on the difference between the molten pool upper surface temperature and the overlying water temperature. In the case of wet in-vessel, for example, the calculated average upward film boiling heat transfer coefficient combined with the thermal radiation emissivity of 0.6 typically ranges from 300 W/m^2K for the temperature difference of 300 K to 900 W/m^2K for the temperature difference of 2000 K. In the case of dry in-vessel, the corresponding thermal radiation heat transfer coefficient ranges from 50 W/m^2K for the temperature difference of 300 K to 600 W/m^2K for the temperature difference of 2000 K. The difference in heat ransfer rate between these two cases is not so much at the molten pool upper surface temperatures of about 2000 K. As shown in Figures 5(a) and 5(b), moreover, the heat transfer rate through the upper surface is much lower than the corresponding heat transfer rate at the outer surface of the vessel coefficient that is placed between 4000 and 5400 W/m^2K in 2500 seconds). The resultant effect of in-vessel coolin gives just a minor effect on the vessel wall temperature transient, comparing with the case of dry in-vessel.

SUMMARY AND CONCLUSIONS

The effect of in- and ex-vessel dual cooling on the retention of an internally heated molten pool confined fully in a hemispherical vessel has been analyzed by using a scale-down reactor vessel and Al_2O_3 melt simulant. An internal power density assumed in the melt simulant was determined by matching the heat flux on the the scale-down vessel wall to estimate from a referenced reactor. Well-known temperature-dependent boiling curves have been applied to the in- and ex-vessel cooling boundaries and radiative heat transfer has been only considered in the case of dry in-vessel. Based on the present configuration of the molten pool and cooling boundaries, the time-varying heat flux distributions and the vessel wall temperature distributions have been obtained through a numerical simulation using the MELTPOOL. The following conclusions can be drawn from this study :

(1) Under the present configuration of the molten pool, the in-vessel cooling gives a small effect to the split fraction of the molten pool heat fluxes regardless of ex-vessel conditions. This is mainly due to the fact that the upward facing boundary cooling condition is more favorable for film boiling with highly reduced heat flux than for nucleate boiling under the present in-vessel cooling condition. In that case, a main mechanism of the heat loss from the upper surface was thermal radiation like the case of dry in-vessel.

(2) Regardless of in-vessel conditions, the entire vessel wall was maintained far below its melting temperature over the whole transient time in the cases of the wet ex-vessel, which was subjected to subcooled nucleate boiling with very high heat flux. At any point on the outer wall, the local heat fluxes do not exceed any of the CHF values evaluated by the existing correlations, which allows very significant margins to the speified CHF value. This means that the present downward heat fluxes from the molten pool are indeed removal and the vessel wall is coolable through nucleate boiling.

(3) Comparing with the case of ex-vessel cooling alone, the in-and ex-vessel cooling provided a minor effect on the vessel wall temperature transient. This is mainly due that the difference in heat ransfer rate between these two cases is not so much at the molten pool upper surface subjected to high temperatures, and moreover the heat transfer rate through the upper surface is much lower than the corresponding heat transfer rate at the outer surface of the vessel.

(4) The amount of boiling heat removal through the overlying water highly depends on the surface temperature of the molten pool and in-vessel pressure, which is determined by a pattern of boiling regime. If the surface temperature of molten pool is reduced to the point that a transition from film

boiling to nucleate boiling is made, the in-vessel cooling will highly effective in removing the molten pool internal heat.

Potential uncertainties have not been considered in the present study, including mutual influence of temperature-dependent melt properties, different configuration of the molten pool (e.g., depth of a molten pool, existence of the overlying particle debris, contact resistance gap cooling), tubulent natural convection flow of the molten pool, change of in-vessel thermal hydraulic condition due to a sustained steam generation, degree of water subcooling and recirculating flow in the vessel outside, and vessel geometrical scale on the in- and ex-vessel dual cooling. More comprehensive influence of these uncertainties on in- and ex-vessel dual cooling must be assessed through further studies.

ACKNOWLEDGMENTS

This study was carried out under the Nuclear R&D Program planned by the Korean Ministry of Science and Technology (MOST).

NOMENCLATURES

c	specific heat capacity ($J/kg\cdot K$)	f	fraction of solidifying melt
$\mathbf{g}$	gravity acceleration (m/s^2)	ΔH	latent heat content (J/kg)
H_l	height of liquid melt (m)	h	enthalpy (J/kg)
K	permeability	L	latent heat of fusion (J/kg)
Nu_{up}	upward Nusselt number	Nu_{dn}	downward Nusselt number
p	pressure (N/m^2)	q''	heat flux (W/m^2)
$\overline{q}''_{avg}$	whole surface-averaged heat flux	q''_{dn}	downward (local) heat flux
$\overline{q}''_{dn}$	downward-averaged heat flux	q''_s	radiative heat loss through upper surface
q''_{up}	upward (local) heat flux	$\overline{q}''_{up}$	upward-averaged heat flux
q'''	volumetric heat source (W/m^3)	R	inner radius of the hemispherical cavity
R'	ratio of the up-to-down heat fluxes	Ra	Rayleigh number ($=\rho^2 g\beta c\Delta T H_l^3/\kappa\mu$) (based on ΔT)
Ra'	modified Rayleigh number (based on q''') ($=\rho^2 cg\beta q''' R^5/\kappa^2\mu$)	S_B	buoyancy source term of natural convection ($=\rho_{ref}\mathbf{g}\beta\cdot(T-T_{ref})$)
S_{dn}	curved surface area of a hemispheric pool	S_h	latent heat source term
S_q	volumetric heat source term	S_u	velocity source terms ($S_u=-\mu\mathbf{u}/K$)
S_{up}	upper surface area of a hemispheric pool	T_m	melting temperature (K)
T_{mp}	molten pool initial temperature (K)	T_s	upper structure temperature (K)
$\mathbf{u}$	velocity vector (m/s)	V_{mp}	volume of a hemispheric pool

Greeks

ρ	liquid density (kg/m^3)	β	thermal expansion coefficient of liquid ($1/K$)
ε_{mp}	molten pool emissivity	κ	thermal conductivity (W/mK)
θ	angle along the vessel wall	μ	dynamic viscosity ($kg/m\cdot s$)

REFERENCES

[1] J.E. O'Brien and G.L. Hawkes, Thermal Analysis of a Reactor Lower Head with Core Relocation and External Boiling Heat Transfer, *AIChE* Symposium Series, **87**, p.159, 1991.
[2] H. Park and V.K. Dhir, Effect of Outside Cooling on the Thermal Behavior of a Pressurized Water Reactor Vessel Lower Head, *Nuclear Technology*, **100**, pp.331-346, 1992.
[3] T.G. Theofanous, C. Liu, S. Additon, S. Angelini, O. Kymalainen, and T. Salmassi, In-vessel Coolability and Retention of a Core Melt, DOE/ID-10460, Vol. 1&2, Center for Risk Studies and Safety, Univ. of California, Santa Barbara, USA, 1995.
[4] T.Y. Chu, J.H. Bentz, S.E. Slezak, and W.F. Pasedag, Ex-vessel Boiling Experiments: Laboratory and Reactor-Scale Testing of the Flooded Cavity Concept for In-vessel Retention, Part II : Reactor-scale boiling experiments of the flooded cavity concept for in-vessel core retention, *Nuclear Engineering and Design,* **169**, p.89, 1997.
[5] F.B. Cheung, Y.C. Liu, Effects of Thermal Insulation on External Cooling of Reactor Vessels under Severe Accident Conditions, CD-ROM publication, NURETH-9, California, USA, 1999.
[6] Special Issue on In-vessel Retention, *Nuclear Engineering and Desig.,* **169** (1-3), pp.1-206, 1997.
[7] I. Szabo, P. Richard, and B. Spindler, Feasibility of an In-vessel Retention Dual System: Functional Analysis and First results, ICONE-6, San Diego, CA, USA, May 10-15, 1998.
[8] KAERI (Korea Atomic Energy Research Institute), Development of Accident Management Guidance for Korean Standard Nuclear Power Plant, KAERI/RR-1939/98, 1999.
[9] B.S. Kim, K.I. Ahn, S.B. Kim, D.H. Kim, A Computational Model for the Analysis of Heat Transfer Characteristics in Liquid Metal Layer under a Solidification Process: MELTPOOL, Proceedings of 8th Intl. Conf. on Nuclear Engineering, ICONE-8, ASME /JSME/SFEN, April 2-6, Baltimore, MD, USA, 2000.
[10] K.I. Ahn, B.S. Kim, S.B. Kim, D.H. Kim, Numerical Analysis of the Heat Transfer Characteristics of a Heat Generating Melt Pool Confined in a Hemispherical Cavity with the MELTPOOL Code, 2nd Japan-Korea Symposium on Nuclear Thermal Hydraulics and Safety (NTHAS-2), Fukuoka, Japan, October 15-18, 2000.
[11] J.H. Ferziger and M. Peric, Computational Methods for Fluid Dynamics, Springer-Verlag, Berlin, Germany, 1996.
[12] H.L. Stone, Iterative Solution of Implicit Approximations of Multidimensional Partial Difference Equations, *SIAM J. Numer. Anal.*, **5**, pp.330-558, 1968.
[13] J.P. Van Doormal and G.D. Raithby, Enhancements of the SIMPLE Method for Predicting Incompressible Fluid Flows, *Numerical Heat Transfer*, **7**. p.147, 1984.
[14] V.R. Voller, and C.R. Swaminathan, General Source-Based Method for Solidification Phase Change, *Numerical Heat Transfer, Part B*, **19**, pp.175-189, 1991.
[15] W.M. Rohsenow and H. Choi, Heat, Mass and Momentum Transfer, Prentice-Hall, Inc, Englewood Cliffs, NJ, 1961.
[16] J.G. Collier, Convective Boiling and Condensation, 2nd Ed., McGraw-Hill, New York, 1981.
[17] S.W. Churchill and R.U. Churchill, A Comprehensive Correlating Equation for Heat and Component Transfer by Free Convection, *Journal of AIChE*, **21**(3), p.604, 1975.
[18] V.K. Dhir, Study of Transitional Boiling Heat Fluxes from Spheres Subjected to Forced Vertical Flow, Intl. Conf. on Heat Transfer, Toronto, Canada, 1978.
[19] K.H. Kang, et al., Experimental Investigations on In-vessel Debris Coolability through Inherent Cooling Mechanisms, Proc. OECD/CSNI Workshop on In-vessel Core Debris Retention and Coolability, NEA/CSNI/R(98)18, pp.251-260, Garching, Germany, March 3-6, 1998.
[20] K.Y. Suh, et al., SONATA-IV Simulation Of Naturally Arrested Thermal Attack In Vessel, Proc. Int. Conf. on PSA Methodology and Applications, pp.453-460, Seoul, Korea, November 26-30, 1995.
[21] M. Epstein and H.K. Fauske, The Three Mile Island Unit 2 Core Relocation – Heat Transfer and Mechanism, *Nuclear Technology*, **87**, pp.1021-1035, 1989.

[22] R.R. Nourgaliev, T.N. Dinh and B.R. Sehgal, Effect of Fluid Number on Heat Transfer Characteristics in Internally Heated Liquid Pools with Raleigh Numbers up to 10^{12}, *Nuclear Engineering and Design*, **169**, pp.165-184, 1997.
[23] N. Zuber, On the Stability of Boiling Heat Transfer, *Trans. ASME*, **80**, p.711, 1958.

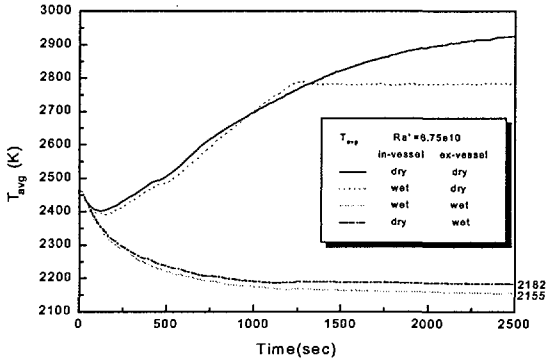

Fig.1. Molten Pool Average Temperature

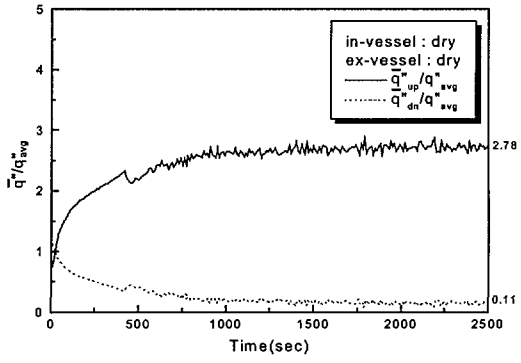

Fig.2(a). Surface-to-Average Heat Flux Ratio : Dry In-vessel and Dry Ex-vessel

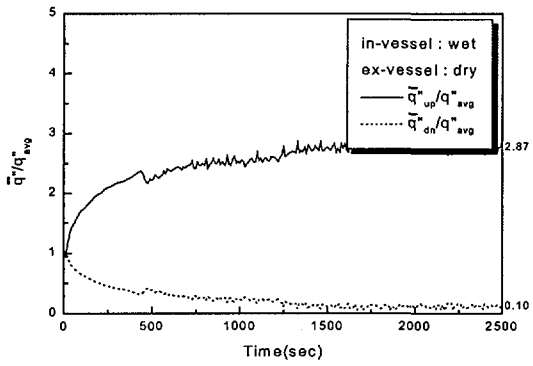

Fig.2(b). Surface-to-Average Heat Flux Ratio : Wet In-vessel and Dry Ex-vessel

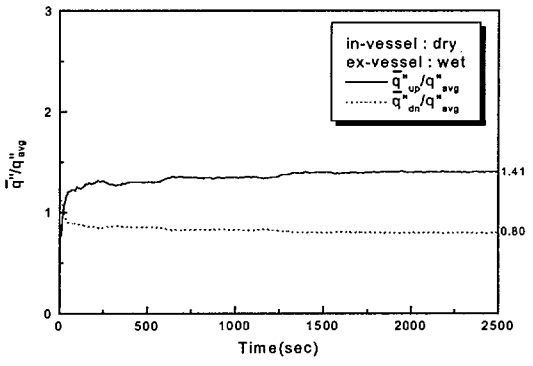

Fig.2(c). Surface-to-Average Heat Flux Ratio : Dry In-vessel and Wet Ex-vessel

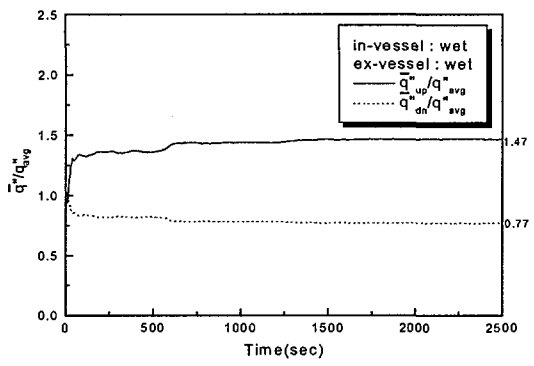

Fig.2(d). Surface-to-Average Heat Flux Ratio : Wet In-vessel and Wet Ex-vessel

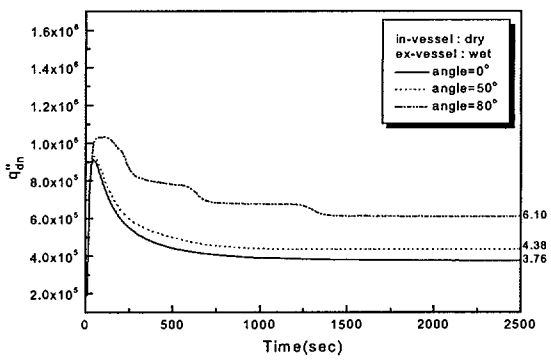

Fig.3(a). Downward Heat Flux with Angular Position at the Outer Surface of the Vessel : Dry In-vessel and Wet Ex-vessel

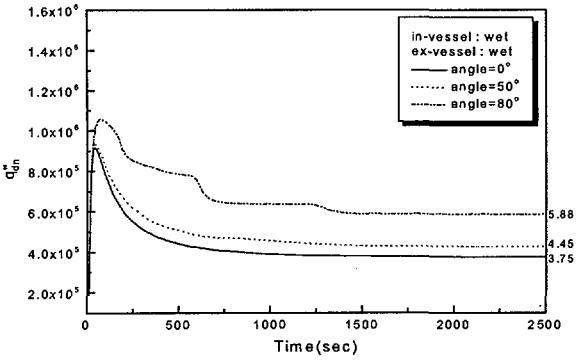

Fig.3(b). Downward Heat Flux with Angular Position at the Outer Surface of the Vessel : Wet In-vessel and Wet Ex-vessel

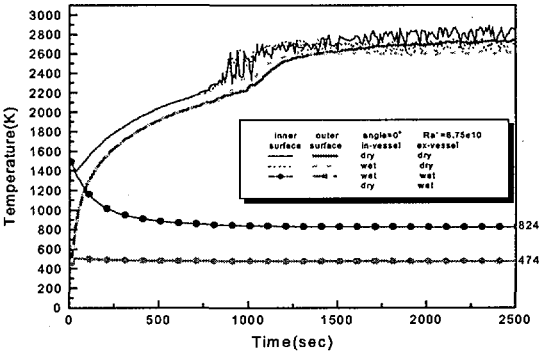

Fig.4(a). Vessel Wall Temperature at Angular Position 0° : Inner and Outer Wall

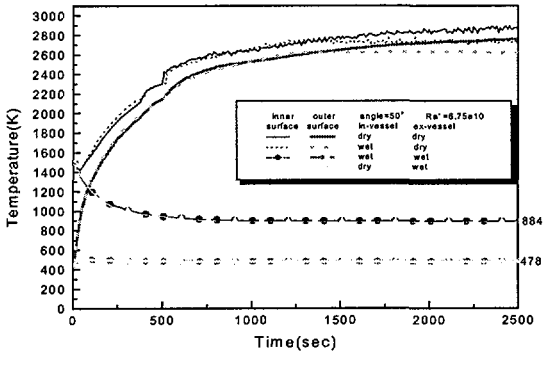

Fig.4(b). Vessel Wall Temperature at Angular Position 50° : Inner and Outer Wall

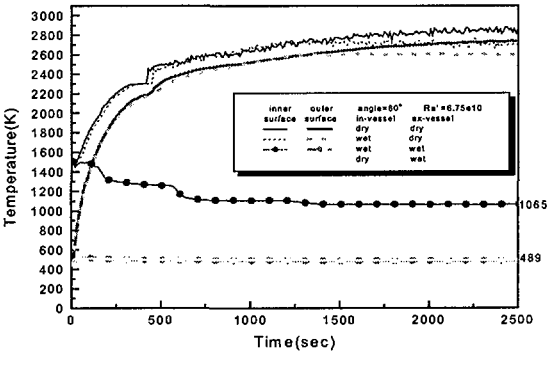

Fig.4(c). Vessel Wall Temperature at Angular Position 80° : Inner and Outer Wall

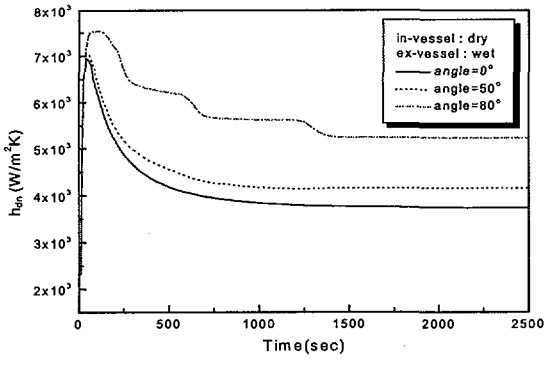

Fig.5(a). Nucleate Boiling Heat Transfer Coefficient at the outside of the vessel : Dry In-vessel and Wet Ex-vessel

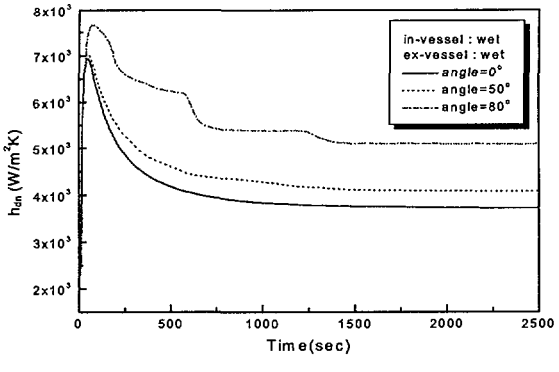

Fig.5(b). Nucleate Boiling Heat Transfer Coefficient at the outside of the vessel : Wet In-vessel and Wet Ex-vessel